

Two-mode squeezed states and entangled states of two mechanical resonators

Fei Xue,^{1,2} Yu-xi Liu,^{1,2} C. P. Sun,³ and Franco Nori^{1,2,4}

¹*CREST, Japan Science and Technology Agency (JST), Kawaguchi, Saitama 332-0012, Japan*

²*Frontier Research System, The Institute of Physical and Chemical Research (RIKEN), Wako-shi, Saitama 351-0198, Japan*

³*Institute of Theoretical Physics, Chinese Academy of Sciences, Beijing, 100080, China*

⁴*Center for Theoretical Physics, Physics Department, Center for the Study of Complex Systems, The University of Michigan, Ann Arbor, Michigan 48109-1040, USA*

(Received 20 February 2007; revised manuscript received 14 June 2007; published 17 August 2007)

We study a device consisting of a dc superconducting quantum interference device (SQUID) with two sections of its loop acting as two mechanical resonators. An analog of the parametric down-conversion process in quantum optics can be realized with this device. We show that a two-mode squeezed state can be generated for two overdamped mechanical resonators, where the damping constants of the two mechanical resonators are larger than the coupling strengths between the dc-SQUID and the two mechanical resonators. Thus we show that entangled states of these two mechanical resonators can be generated.

DOI: [10.1103/PhysRevB.76.064305](https://doi.org/10.1103/PhysRevB.76.064305)

PACS number(s): 03.67.Mn, 85.25.Dq

I. INTRODUCTION

Motivated by their relevance to quantum information, coherent quantum behavior of macroscopic solid-state devices are of great interest. Quantized energy levels, coherent time evolution, superposition, and entangled states—have all been observed in various solid-state devices, such as quantum dots and superconducting quantum interference devices (SQUIDs). Nanomechanical resonators (NAMRs)^{1–4} with frequencies as high as Giga-Hertz can now be fabricated.^{5–8} At milli-Kelvin temperatures, such mechanical resonators are expected to exhibit coherent quantum behavior.

In order to detect and control mechanical resonators, some transducer methods must be used. These include optical methods, magnetomotive techniques, and couplings to single electron transistors.^{1–4} A design of mechanical qubits based on buckling nanobars was recently studied in Ref. 9. Also, buckled modes analogous to buckled-bars have been proposed for magnetic nanostructures,¹⁰ and mechanical bars bent by electric fields have been considered, e.g., Ref. 11. Moreover, these quantum mechanical nanobars can exhibit behavior similar to superconducting quantum circuits.¹²

The quantization of NAMRs has been studied by coupling NAMRs to a superconducting charge qubits.^{13–17} By controlling the charge qubit, a NAMR can be prepared into different quantum states. Also, charge qubits can be used to measure the quantum states of the NAMRs. Quantum nondemolition measurements of a NAMR were studied with an rf-SQUID acting as a transducer between the NAMR and an LC resonator.¹⁸ It was shown that a strong coupling cavity QED regime can be realized for a NAMR and a superconducting flux qubit¹⁹ or a NAMR with a magnetic tip coupled to an electron spin.²⁰

For their usages of sensitive displacement detection beyond the standard quantum limit, single-mode squeezed states of a nanomechanical resonator were theoretically studied. It was shown that squeezed states of the nanomechanical resonator can be generated by either periodically flipping a superconducting charge qubit coupled to it²¹ or by measuring the superconducting charge qubit coupled to it.²² The squeez-

ing of the nanoresonator state can also be produced by periodically measuring its position by a single-electron transistor.²³

Two-mode squeezed states, when these two modes are from two spatially separated macroscopic objects, are macroscopic entangled states. The generation of these entangled states of macroscopic objects is of fundamental interest. Several protocols have been proposed to entangle two tiny mirrors with the assistance of photons.^{24,25} Here we study a device consisting of a dc-SQUID with two opposite sections of the SQUID loop suspended from the substrate. The suspended parts, shaped as doubly-clamped beams, can be approximated as NAMRs. The magnetic flux threading the loop of the dc-SQUID is modulated by the displacements of both NAMRs. Then the dynamics of the dc-SQUID is modified by the NAMRs. We study how the potential energy of the dc-SQUID is modified by the displacement of the NAMRs. We show that the nonlinear coupling between a dc-SQUID and the NAMRs, where the dc-SQUID is approximated as a quantum harmonic oscillator, offers a flexible method for the detection and control of NAMRs. Specifically, we discuss two-mode squeezed states of these two NAMRs through an analog of the two-mode parametric down-conversion process in quantum optics. We show here that two-mode squeezed states of the two NAMRs can be obtained even when the couplings between the dc-SQUID and the two NAMRs are weaker than their damping rates. In contrast to this, for the proposal studied in Ref. 26 the entanglement between the NAMRs decreases rapidly with time. Other forms of squeezing of mechanical oscillators (phonons) have been studied about a decade ago in Refs. 27–30.

This paper is organized as follows. At the beginning of Sec. II our device is described. Then, after we study the potential energy of the dc-SQUID, the Hamiltonian of the device is presented. The interaction Hamiltonian between a dc-SQUID and two NAMRs is complicated and has many terms. However, if the frequency of the dc-SQUID is properly chosen by the bias current of the dc-SQUID, then only a few terms dominate the dynamics of the coupled system, which is illustrated by writing the interaction Hamiltonian in the interaction picture. Then, in Sec. III we study a special

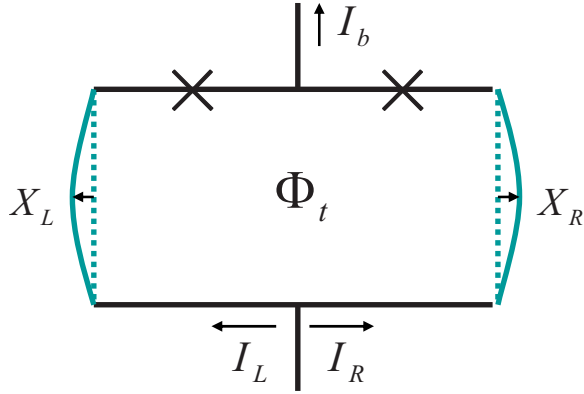


FIG. 1. (Color online) Schematic diagram of the top view of the device considered here. It consists of a rectangular-shaped dc-SQUID and two mechanical resonators shown in blue on the left and right sides. These two opposite segments of the dc-SQUID are freely suspended and are treated as two nanomechanical resonators (NAMRs). The dotted lines indicate the equilibrium positions of the left and right NAMRs. Each “X” in the top segment of the loop represents a Josephson junction. X_L (X_R) is the displacement of the center of the left (right) resonator. The two NAMRs could be located sufficiently “far apart” by using a SQUID with an appropriate aspect ratio. This could provide EPR-type correlations on the two NAMRs located sufficiently “far apart” for wide-enough SQUIDs.

case where, under an appropriate choice of the parameters, the interaction Hamiltonian is simplified to study the two-mode parametric down-conversion process in the device. Squeezed states of the two NAMRs are studied by the Heisenberg-Langevin method. Conclusions are given in Sec. IV.

II. COUPLING A dc SQUID WITH TWO NANOMECHANICAL RESONATORS

The device we studied is schematically illustrated in Fig. 1. It consists of a dc-current-biased SQUID with rectangular shape and with two mechanical resonators. The left and right sides of the SQUID are suspended from the substrate and form the two mechanical oscillators, our NAMRs. We assume here that these two doubly-clamped beams vibrate in their fundamental flexural modes and in the plane of the SQUID loop. We use the following notations I_L (I_R) for the current in the left (right) Josephson junction, and φ_L (φ_R) for the phase drop across the left (right) Josephson junction. The two Josephson junctions are assumed to be identical and have the same critical current I_c . Thus the bias current I_b of the dc-SQUID has the form

$$I_b = I_c(\sin \varphi_L + \sin \varphi_R). \quad (1)$$

We assume that the inductance of the dc-SQUID loop is negligibly small, and thus the magnetic energy of the circulating current in the dc-SQUID loop is neglected. Thus the voltage drop over the two junctions is zero. Therefore, $\varphi_R - \varphi_L = \varphi_t$, where φ_t is the phase related to total magnetic flux Φ_t threading the dc-SQUID loop

$$\varphi_t = 2\pi \frac{\Phi_t}{\Phi_0}. \quad (2)$$

Here $\Phi_0 = h/2e$ is flux quantum. Introducing two new variables

$$\varphi = \frac{1}{2}(\varphi_R + \varphi_L), \quad (3a)$$

$$\varphi_- = \frac{1}{2}(\varphi_R - \varphi_L), \quad (3b)$$

and taking into account that $\varphi_- = \varphi_t/2$, the bias current in Eq. (1) can be written as

$$I_b = 2I_c \sin \varphi \cos \frac{\varphi_t}{2}. \quad (4)$$

It is here assumed that X_L (X_R) is the amplitude for the fundamental flexural mode of the left (right) beam. Let B_L (B_R) be the magnetic field normal to the plane of the SQUID loop near the left (right) mechanical beam and Φ_b the external applied magnetic flux threading perpendicularly the dc-SQUID loop when $X_L = X_R = 0$. It is assumed that B_L (B_R) is constant in the oscillating region of the left (right) beam. Then, the total magnetic flux threading the dc-SQUID loop is given by

$$\Phi_t = \Phi_b + \Phi_X, \quad (5)$$

where Φ_X is the additional magnetic flux when the two NAMRs are displaced from their equilibrium positions

$$\Phi_X = B_L X_L l + B_R X_R l. \quad (6)$$

Here, l is the effective length of the left and right beam. l is defined as $l \equiv S_L/X_L$, where S_L is the area between the equilibrium position of the NAMR and its bent configuration. Namely, the area S_L spans the region between the blue dashed line and the blue bent line in Fig. 1. Equation (6) indicates that the variables of the two NAMRs enter in the dynamics of the dc-SQUID by influencing the flux threading the dc-SQUID. The influence of the two NAMRs on the dynamics of the SQUID can also be revealed quantitatively in the potential energy of the dc-SQUID, since this is also a function of the displacements of the two NAMRs. Thus, we first study the potential energy of the SQUID and afterwards the entire Hamiltonian of the coupled system.

A. Potential energy of the vibrating dc-SQUID

The potential energy of the dc-SQUID is

$$U(\varphi, \Phi_X) = -2E_J \cos\left(\pi \frac{\Phi_b}{\Phi_0} + \pi \frac{\Phi_X}{\Phi_0}\right) \cos \varphi - \frac{I_b}{I_c} E_J \varphi, \quad (7)$$

where $E_J = \hbar I_c / (2e)$ is the Josephson energy of the junction.^{31,32} To have an idea of the situation under which the dc-SQUID can be described by a quasiparticle in a quadratic potential, in Figs. 2(a)–2(d) we plot this potential energy (7)

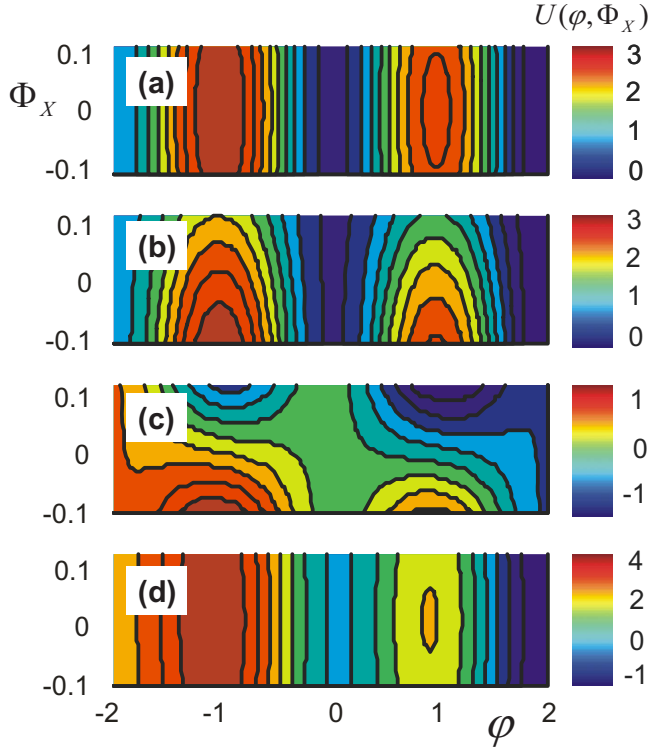


FIG. 2. (Color online) The potential energy $U(\varphi, \Phi_X)$ (scaled by E_J) of the dc-SQUID as a function of the phase variable φ and the magnetic flux Φ_X originating from the displacements of the two NAMRs. The red color represents higher potential energy U , and the blue color represents lower potential energy. Both φ and Φ_X are shown in units of π/Φ_0 . In (a)–(c), the bias magnetic flux Φ_b threading the loop of the dc-SQUID is set at $2n\Phi_0$, $(2n+\frac{1}{4})\Phi_0$, and $(2n+\frac{1}{2})\Phi_0$, respectively; and the bias currents are all set at $I_b = 0.1I_c$. In (d), $\Phi_b = 2n\Phi_0$ and $I_b = 0.5I_c$.

for various values of the bias magnetic flux Φ_b and the bias current I_b . Since $\Phi_X/\Phi_0 \ll 1$ in the case of experiments using a GHz NAMR, here we focus on the limit $\Phi_X/\Phi_0 < 0.1$ in Fig. 2. A particle in a quadratic potential can be described by a harmonic oscillator when its kinetic energy is much smaller than the barrier of the potential. We notice that, for the bias magnetic flux $\Phi_b = 2n\Phi_0$, with n being an integer, the phase variable φ falls in a potential well when the NAMRs oscillate around their equilibrium points. It is possible to approximate the dynamics of φ as a harmonic oscillator. The charging energy of the dc-SQUID $E_c \equiv (2e)^2/(2C_J)$ is assumed here to be much smaller than the modified Josephson energy $(\cos q_0)E_J$ of the dc-SQUID. Here, $q_0 = \sin^{-1}(I_b/2I_c)$ is a value of φ which corresponds to one of the minima of the potential energy $U(\varphi, \Phi_X)$, when the two NAMRs are at their equilibrium positions. C_J is the capacitance of the left and right Josephson junctions.

We then expand the potential $U(\varphi, \Phi_X)$ near one of its minimum points $(\varphi, \Phi_X) = (q_0, 0)$. When $\Phi_X/\Phi_0 \ll 1$ and $\Phi_b = 2n\Phi_0$, the first cosine in Eq. (7) depends weakly on Φ_X . Up to second order in Φ_X and φ , and after shifting the origin of φ to q_0 , and omitting the constant terms, the potential energy in Eq. (7) becomes

$$U(\varphi, \Phi_X) = E_J(\cos q_0)\varphi^2 - E_J(1 - \cos q_0)\left(\pi\frac{\Phi_X}{\Phi_0}\right)^2 - E_J\left[\sin q_0\varphi + \frac{1}{2}(\cos q_0)\varphi^2\right]\left(\pi\frac{\Phi_X}{\Phi_0}\right)^2. \quad (8)$$

Therefore, if the first term in the above potential is much larger than the other two terms, the dynamics of φ will still be well described by a harmonic oscillator.

The higher order terms, such as $\pi^4\Phi_X^4/(24\Phi_0^4)$, in the expansion of $\cos(\pi\Phi_X/\Phi_0)$ are negligibly small for the situation considered in our paper, when $\Phi_X/\Phi_0 \approx 10^{-3}$. Theoretically, it is possible to increase the ratio $\pi\Phi_X/\Phi_0$ by using a stronger magnetic field B_L and B_R and/or using soft NAMRs with greater zero-point fluctuations. However, in practice, the magnetic field is limited to at most tens of Tesla and the zero-point fluctuations of the NAMRs are less than 10^{-12} m for the most of the experiments. Therefore, the periodic nature of the Josephson Hamiltonian has no chance to play a role here. Indeed the situation considered here is very similar to the optical parametric-down-conversion system, except for the coefficients of polynomial expansions of the interaction Hamiltonian.

Now we consider how well a dc-SQUID is approximated by a harmonic oscillator. Since the barrier of the potential $U(\varphi, \Phi_X)$ has a finite height, the dynamics of φ is not an ideal harmonic oscillator. However, if the energy of the quasiparticle is small enough, the dynamics of φ can be approximately described by a harmonic oscillator. The maximum number N_{\max} of energy levels that can be confined in the potential $U(\varphi, 0)$ is $N_{\max} \equiv \Delta U/\Omega$, where the height of the potential is

$$\Delta U = 2E_J[2\cos q_0 + \sin q_0(2q_0 - \pi)], \quad (9)$$

and Ω is the frequency of the harmonic oscillator.

B. Hamiltonian of the coupled system

Near the minimum potential $U(q_0, 0)$, the free Hamiltonian of the dc-SQUID can be written as a harmonic oscillator Hamiltonian

$$\frac{H_s}{\hbar} = E_c\dot{\varphi}^2 + E'_J\varphi^2, \quad (10)$$

with

$$E'_J = E_J \cos q_0, \quad (11)$$

where the constant term has been omitted when we derived the Hamiltonian in Eq. (10). It is convenient to introduce the annihilation and creation operators a and a^\dagger :

$$a = \left(\frac{E'_J}{E_c}\right)^{1/4} \varphi + i\left(\frac{E_c}{E'_J}\right)^{1/4} \dot{\varphi}, \quad (12a)$$

$$a^\dagger = \left(\frac{E'_J}{E_c}\right)^{1/4} \varphi - i\left(\frac{E_c}{E'_J}\right)^{1/4} \dot{\varphi}. \quad (12b)$$

Then the free Hamiltonian in Eq. (10) of the dc-SQUID can be rewritten in the form

$$H_s = \hbar\Omega a^\dagger a, \quad (13)$$

with the angular frequency

$$\Omega = \sqrt{E_c E'_J}. \quad (14)$$

When the energy of the dc-SQUID is not very large ($\langle a^\dagger a \rangle < N_{\max}$), the dynamics of φ is well described by a harmonic oscillator under a suitable bias magnetic flux threading the loop of the dc-SQUID. It is convenient to also introduce annihilation and creation operators for the fundamental flexural modes of the two NAMRs ($i=L, R$)

$$b_i = \sqrt{\frac{m_i \omega_i}{2\hbar}} X_i + i \sqrt{\frac{1}{2\hbar m_i \omega_i}} P_i, \quad (15a)$$

$$b_i^\dagger = \sqrt{\frac{m_i \omega_i}{2\hbar}} X_i - i \sqrt{\frac{1}{2\hbar m_i \omega_i}} P_i. \quad (15b)$$

Here, X_i and P_i are the coordinate and momentum operators of the i th NAMR and m_i and ω_i are the effective mass and angular frequency of the i th NAMR. The effective angular frequency ω_i is not the one of the fundamental flexural mode, which is modified by the second term in the potential (8). Then the free Hamiltonian of the two NAMRs can be written in the form

$$H_{\text{NAMR}} = \hbar\omega_L b_L^\dagger b_L + \hbar\omega_R b_R^\dagger b_R, \quad (16)$$

where the constant terms have been omitted. Thus, in terms of creation and annihilation operators, from Eq. (8), the *interaction* Hamiltonian between these two NAMRs and the dc-SQUID are given by

$$V = -[g_L(b_L + b_L^\dagger) + g_R(b_R + b_R^\dagger)]^2 \times [c_1(a + a^\dagger) + c_2(a + a^\dagger)^2], \quad (17)$$

where

$$g_L = \frac{\pi B_L l}{\Phi_0} \sqrt{\frac{\hbar}{2m_L \omega_L}}, \quad (18a)$$

$$g_R = \frac{\pi B_R l}{\Phi_0} \sqrt{\frac{\hbar}{2m_R \omega_R}}, \quad (18b)$$

$$c_1 = \frac{\Omega}{2} (\tan q_0) \left(\frac{E_J \cos q_0}{E_c} \right)^{1/4}, \quad (18c)$$

$$c_2 = \frac{\Omega}{8}. \quad (18d)$$

The interaction Hamiltonian (17) is central to this work. Notice that it contains both linear and nonlinear terms. Generally, it is very difficult to evaluate the behavior of this coupled system. However, since the frequency Ω of the dc-SQUID can be set by the bias current I_b , we can reduce the interaction Hamiltonian V in Eq. (17) to a simplified form by invoking the rotating wave approximation. We now rewrite the interaction Hamiltonian V in Eq. (17) in the interaction picture, with the free Hamiltonian

TABLE I. Terms in the interaction Hamiltonian (17) and their frequencies, in the interaction picture.

	Frequencies	Interaction terms
0	0	$\frac{1}{2}c_2(g_L^2 b_L^\dagger b_L + g_R^2 b_R^\dagger b_R)a^\dagger a$,
1	$2\omega_L$	$c_2 g_L^2 b_L^2 a^\dagger a$,
2	$2\omega_R$	$c_2 g_R^2 b_R^2 a^\dagger a$,
3	$\omega_L + \omega_R$	$c_2 g_L g_R b_L b_R a^\dagger a$,
4	$\omega_L - \omega_R$	$c_2 g_L g_R b_L^\dagger b_R^\dagger a^\dagger a$,
5	2Ω	$c_2(g_L^2 b_L^\dagger b_L + g_R^2 b_R^\dagger b_R)a^2$,
6	Ω	$c_1(g_L^2 b_L^\dagger b_L + g_R^2 b_R^\dagger b_R)a$,
7	$2\omega_L + 2\Omega$	$c_2 g_L^2 b_L^2 a^2$,
8	$2\omega_L - 2\Omega$	$c_2 g_L^2 b_L^2 a^{\dagger 2}$,
9	$2\omega_R + 2\Omega$	$c_2 g_R^2 b_R^2 a^2$,
10	$2\omega_R - 2\Omega$	$c_2 g_R^2 b_R^2 a^{\dagger 2}$,
11	$\omega_L + \omega_R + 2\Omega$	$c_2 g_L g_R b_L b_R a^2$,
12	$\omega_L + \omega_R - 2\Omega$	$c_2 g_L g_R b_L b_R a^{\dagger 2}$,
13	$\omega_L - \omega_R + 2\Omega$	$c_2 g_L g_R b_L b_R^\dagger a^2$,
14	$\omega_L - \omega_R - 2\Omega$	$c_2 g_L g_R b_L b_R^\dagger a^{\dagger 2}$,
15	$2\omega_L + \Omega$	$c_1 g_L^2 b_L^2 a$,
16	$2\omega_L - \Omega$	$c_1 g_L^2 b_L^2 a^\dagger$,
17	$2\omega_R + \Omega$	$c_1 g_R^2 b_R^2 a$,
18	$2\omega_R - \Omega$	$c_1 g_R^2 b_R^2 a^\dagger$,
19	$\omega_L + \omega_R + \Omega$	$c_1 g_L g_R b_L b_R a$,
20	$\omega_L + \omega_R - \Omega$	$c_1 g_L g_R b_L b_R a^\dagger$,
21	$\omega_L - \omega_R + \Omega$	$c_1 g_L g_R b_L b_R^\dagger a$,
22	$\omega_L - \omega_R - \Omega$	$c_1 g_L g_R b_L b_R^\dagger a^\dagger$,

$$H_0 = \hbar\Omega a^\dagger a + \hbar\omega_L b_L^\dagger b_L + \hbar\omega_R b_R^\dagger b_R. \quad (19)$$

Then the terms of the interaction Hamiltonian V can be classified by the ways that the frequencies ω_L , ω_R , and Ω can be combined. In Table I, we list half of the coupling terms and the combinations of their frequencies. The other half are their corresponding Hermitian conjugate terms, which have the same frequencies but with a negative sign.

In Table I, it can be seen that, for large detuning, one needs to mainly consider the zero-frequency terms in the first row of the table. Then this interaction Hamiltonian V enables a quantum nondemolition measurement of discrete Fock states of a NAMR, as discussed in Ref. 18. When the frequency of the dc-SQUID is set at some special value, one can mainly consider the resonant terms. For example, if the frequency of the dc-SQUID and those of the two NAMRs are properly set so that $\Omega \neq \omega_L = \omega_R$ and also $\Omega \neq 2\omega_L = 2\omega_R$, then only the zero-frequency terms and resonant terms in the interaction Hamiltonian V are kept under the rotating wave approximation. The reduced interaction Hamiltonian V_r consists of the terms

$$V_r = c_2 g_L g_R b_R^\dagger b_L a^\dagger a + \text{H.c.}, \quad (20)$$

which in fact offers us a mechanism for coupling two NAMRs. Thus, our proposed device offers a flexible (literally) model for the control and measurement of NAMRs.

III. TWO-MODE SQUEEZED STATES OF TWO NANOMECHANICAL RESONATORS

In this section we focus on the two-mode squeezed states of the two NAMRs. It is possible to produce entangled states of the two NAMRs by considering the analog of the parametric down-conversion in quantum optics. The zero-frequency terms in Table I commute with the free Hamiltonian (13) of the dc-SQUID and the free Hamiltonian (16) of the two NAMRs. Let us assume that the proposed circuit works at low temperature. If the two NAMRs are initially in the vacuum state or in very low-energy states, then we have $\delta_{LR} \ll \Omega$, with

$$\delta_{LR} = c_2(g_R^2 \langle b_R^\dagger b_R \rangle + g_L^2 \langle b_L^\dagger b_L \rangle). \quad (21)$$

Then we can rewrite the free Hamiltonians of the dc-SQUID Eq. (13) and the two NAMRs Eq. (16) as

$$H'_0 = \Omega' a^\dagger a + \omega_L b_L^\dagger b_L + \omega_R b_R^\dagger b_R, \quad (22)$$

where $\Omega' = \Omega - \delta_{LR}$. By properly setting the bias current I_b one can let $\Omega' - \omega_L - \omega_R = 0$. Then, in the interaction picture, after adopting the rotating wave approximation, we simplify the interaction Hamiltonian between two NAMRs and dc-SQUID as

$$V' = \eta(a^\dagger b_L b_R + a b_L^\dagger b_R^\dagger), \quad (23)$$

where

$$\eta = -c_1 g_L g_R. \quad (24)$$

Driven by this interaction Hamiltonian V' , two-mode squeezed states of the two NAMRs can be produced in the device similarly to a light beam interacting inside a nonlinear medium in quantum optics, because both of them follow the *same* Hamiltonian (23).

We now consider that the mode of the dc-SQUID is in a coherent state $|\alpha\rangle$, where $|\alpha| \gg 1$. Then we can treat the mode of the dc-SQUID as a classical field and replace the operator a in the Hamiltonian V' in Eq. (23) by a complex number $|\alpha| \exp(-i\phi)$. Then, in the interaction picture defined by the Hamiltonians (22) and (23), the dynamics of the coupled system is described by the following Hamiltonian:

$$V_I = e^{i\phi} |\alpha| \eta b_L b_R + e^{-i\phi} |\alpha| \eta b_L^\dagger b_R^\dagger. \quad (25)$$

The motions of b_L and b_R are

$$b_L(t) = \cosh(\gamma) b_L - i e^{-i\phi} \sinh(\gamma) b_R^\dagger, \quad (26a)$$

$$b_R(t) = \cosh(\gamma) b_R - i e^{-i\phi} \sinh(\gamma) b_L^\dagger, \quad (26b)$$

in the interaction picture of the Hamiltonians (22) and (25), with

$$\gamma = |\alpha| \eta t. \quad (27)$$

The generation of two-mode squeezed states of these two NAMRs can be shown by their collective coordinate and momentum operators

$$X_T(t) = X_L(t) + X_R(t), \quad (28a)$$

$$P_T(t) = P_L(t) + P_R(t), \quad (28b)$$

where $X_i(t)$ and $P_i(t)$, $i=L,R$, are defined by Eq. (15) by substituting b_i and b_i^\dagger with $b_i(t)$ and $b_i^\dagger(t)$ in Eq. (26). The uncertainty relation for the collective coordinate and momentum operators $X_T(t)$ and $P_T(t)$ is

$$\Delta[X_T(t)] \Delta[P_T(t)] = \hbar |\cosh^2 \gamma + e^{2i\phi} \sinh^2 \gamma|. \quad (29)$$

In Eq. (29) we have assumed that the zero-point fluctuation of positions of the left NAMR

$$\delta_L = \sqrt{\hbar/(2m_L \omega_L)}, \quad (30)$$

and that of the right NAMR

$$\delta_R = \sqrt{\hbar/(2m_R \omega_R)} \quad (31)$$

are the same. Here

$$\delta_X = \sqrt{2} \delta_L = \sqrt{2} \delta_R \quad (32)$$

is defined as the zero-point fluctuation of the collective coordinates X_T of the two NAMRs.

If we choose $\phi = -\pi/2$, then the variance of the collective coordinates $X_T(t)$ becomes

$$\Delta[X_T(t)] = \delta_X \exp(\gamma). \quad (33)$$

Notice that $\gamma < 0$ because $\gamma = -c_1 g_L g_R |\alpha| t$. Therefore, perfect two-mode squeezed states, i.e., pure entangled states, of the two NAMRs are generated.

The variance of $X_T(t)$ (the entanglement) was obtained above by assuming that both the left and right NAMRs be in their ground states. It can be checked that if both the left and right NAMRs are initially in coherent states or thermal states, then the Hamiltonian (25) will not produce entangled states of them. However, if only one of the NAMRs is initially prepared into a number state, then entangled states of these two NAMRs can be generated by the Hamiltonian (25). For example, when the left and the right NAMRs are initially prepared in the number states $|0\rangle$ and $|1\rangle$, respectively, then the Bell-type entangled state $a_1|01\rangle + a_2|10\rangle$ can be generated. Here, a_1 and a_2 are complex numbers. When one of the two NAMRs is initially in a coherent state and the other one is in the vacuum state, then the so-called ‘‘single-photon-added coherent states’’³³ can be generated by the Hamiltonian (25).

Let us now consider the more realistic case where both the dc-SQUID and the two NAMRs are coupled to their environments. The quality factors of the two NAMRs with GHz frequency are smaller than that of the dc-SQUID.^{6,34} The quality factor of a GHz NAMR is of the order of 10^3 , while that of a superconducting circuit can be as large as 10^6 . Therefore, below we consider the noise from the environment acting on the two NAMRs. To include damping effects, due to the noise from the environments, on the dynamics of the two NAMRs, we use the Heisenberg-Langevin equation method.³⁵ Then, for the motions of the operators of the NAMRs, we have the following set of equations:

$$\frac{d}{dt} b_L = -\xi b_L^\dagger - \frac{\kappa_L}{2} b_L + F_L(t), \quad (34a)$$

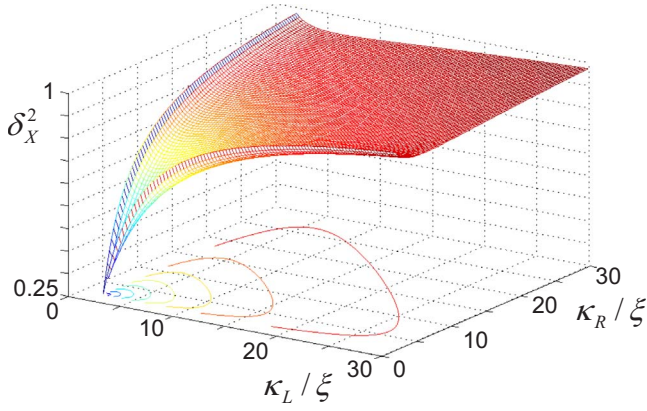


FIG. 3. (Color online) The squared variance of the collective coordinates X_T of the two NAMRs as the function of damping rates κ_L and κ_R of the left and right NAMRs, both κ_L and κ_R are normalized by the effective coupling constant ξ . Here, δ_X is the zero fluctuation of the collective coordinates of the two NAMRs.

$$\frac{d}{dt}b_R = -\xi b_L^\dagger - \frac{\kappa_R}{2}b_R + F_R(t). \quad (34b)$$

As in the ideal case in Eq. (33) we also let $\phi = -\pi/2$. Here,

$$\xi = |\alpha|\eta \quad (35)$$

is the effective coupling strength between the dc-SQUID and two NAMRs. Also, κ_L and κ_R represent the damping rates of the left and right NAMRs, respectively; and the associated noise operators are $F_L(t)$ and $F_R(t)$. We evaluate the properties of the states of the two NAMRs by the variance of the collective coordinates X_T . We find that the damping of the two NAMRs help producing two-mode squeezed states of the two NAMRs, regardless of the initial states. The variance of the collective coordinates X_T is calculated as

$$[\Delta(X_T)]^2 = \frac{\delta_L^2}{\kappa_+}(2\kappa_R\Delta_\xi + \kappa_-) + \frac{\delta_R^2}{\kappa_+}(2\kappa_L\Delta_\xi - \kappa_-) - 8\frac{\delta_L\delta_R}{\kappa_+}\xi\Delta_\xi \quad (36)$$

under the Markov approximation and in the overdamped case, $\xi < \kappa_L/2$ and $\xi < \kappa_R/2$. In the Appendix we outline the main ideas of the derivation. Here,

$$\kappa_\pm = \kappa_L \pm \kappa_R, \quad \Delta_\xi = \frac{\kappa_L\kappa_R}{\kappa_L\kappa_R - 4\xi^2}. \quad (37)$$

When the zero-point fluctuations of the left and right NAMRs are equal, we have

$$[\Delta(X_T)]^2 = \frac{\delta_X^2}{4}\Delta_\xi \left(1 - \frac{4\xi}{\kappa_L + \kappa_R}\right). \quad (38)$$

Figure 3 shows the variance of the collective coordinates X_T versus the damping rates κ_L and κ_R . It is clear from Fig. 3 that appreciable squeezing can be generated even when the dampings of the two NAMRs are severe (ten times the coupling constant ξ). This indicates that the squeezing is robust against damping of the NAMRs. The maximum squeezing is obtained when both damping rates (for the left and right

NAMRs) approach the coupling strength between them and the dc-SQUID. Since the coupling strength ξ is proportion to $|\alpha|$, one can increase the squeezing rate by gradually increasing the power of the microwave applied to the dc-SQUID. As the damping rates of the two NAMRs increase, the squeezing effect decreases steadily.

To consider the experimental feasibility of our proposal, we choose the following parameters for the two NAMRs and the dc-SQUID

$$m_L = m_R = 10^{-18} \text{ Kg}, \quad (39a)$$

$$\omega_L = 1.5 \text{ GHz}, \quad (39b)$$

$$\omega_R = 1.2 \text{ GHz}, \quad (39c)$$

$$l = 10 \text{ }\mu\text{m}, \quad (39d)$$

$$B_L = B_R = 1 \text{ T}, \quad (39e)$$

$$\kappa_L = \kappa_R = 2 \text{ MHz}, \quad (39f)$$

$$E_C = 0.061 \text{ GHz}, \quad (39g)$$

$$E_J = 120 \text{ GHz}. \quad (39h)$$

It was already demonstrated in experiments^{6,36} that a 10 μm long doubly clamped beam can oscillate with a frequency of several GHz. The effective mass of this antenna-shaped beam is much smaller than its weight. And its effective mass can be further modified when the beams are under strains and stresses. The numbers used here for the dc-SQUID are also consistent with the experimental numbers shown in Ref. 37. Then the additional magnetic flux from the two NAMRs, $\Phi_X/\Phi_0 \approx 5 \times 10^{-3} \ll 1$, would satisfy our assumption in Sec. II. The maximum number N_{\max} of energy levels confined in the current biased potential energy is calculated as $N_{\max} \approx 150$. Therefore, the harmonic oscillator approximation and the classical field approximation for the dc-SQUID are both possible. The time needed to obtain the two-mode squeezed state is determined by the effective coupling constant ξ . Assuming the same damping rates for the two NAMRs, the maximum squeezing $\Delta(X_T) = (1/2)\delta_X$ can be obtained. Therefore, it should be possible to realize our proposal of generating two-mode squeezed states of the two NAMRs with current experimental conditions.

To experimentally detect the generated two-mode squeezed state of the two NAMRs, a (in principle) relatively direct method would be checking the variance of the collective coordinate X_T of the two NAMRs. Since the left and right NAMRs are symmetric in the interaction Hamiltonian (17), they can be treated as one virtual NAMR. To detect two-mode squeezed states of the two NAMRs, the detection methods should be able to approach standard quantum limit of the NAMRs. With traditional displacement detection methods,^{1,4,39-41} such as optical interferences, magnetic-motive method, and coupled single electron transistor, the best record of detection precision was about 4.3 standard quantum limits.³⁸ There are also other proposals for displace-

ment detection by coupling the mechanical oscillator to some two level system.^{13,19,21} These methods, in principle, can detect quantum states of the NAMRs. After the entangled state is generated, one can switch the dc-SQUID to the phase qubit regime,⁴² and utilize the nonlinear coupling between the virtual NAMR and the dc-SQUID. Then the SQUID can be used to measure the variance of X_T , as discussed in Ref. 21.

IV. DISCUSSIONS AND CONCLUSIONS

In our proposal, we only consider the fundamental vibration modes of the NAMRs. Generally, there are also vibration modes with higher frequencies, torsional and strain-stress oscillations in the NAMRs.¹ The vibration modes with higher frequencies will be excited only when they happen to resonate with the dc-SQUID, which can be easily avoided by optimizing the parameters of the NAMRs. As for torsional and strain-stress oscillations, they are hardly coupled to the dc-SQUID. These modes of oscillations of the NAMRs will not change the magnetic flux through the dc-SQUID, thereby these modes cannot be coupled to the dc-SQUID, even through their frequencies match the resonant condition. It is similar to the case of the experiments of magnetomotive detection of flexural oscillation of NAMRs,¹ where torsional and strain-stress oscillations have been neglected.

As mentioned in Sec. III, to generate two-mode squeezed states of NAMRs, the NAMRs should start in their ground states or number states. The NAMRs should be cooled such that the thermal excitation energy is less than those corresponding to the NAMRs' frequencies. For a one-GHz NAMR, this means that the temperature should be below 50 mK, which is still within the capability of dilution refrigerators. In principle, it is possible to prepare the NAMRs used in our proposal in their ground states. Moreover, recently there have been many efforts in reducing the temperature of mechanical resonators by active cooling.⁴³⁻⁴⁷ Also a temperature as low as 5 mK was already demonstrated for a mechanical resonator.⁴⁷ In addition, there are also theoretical proposals for the production of number states of NAMRs.⁴⁸ Therefore, though currently the ground states and (or) number states of NAMRs might be difficult to prepare experimentally, we expect these to be realized more earlier in the near future. For example, if the temperature of a GHz NAMR reaches 10 mK, the thermal occupation number will be $\sim 10^{-3}$, which is nearly a ground state.

In conclusion, we have proposed a device to couple a dc-SQUID to two NAMRs, which can be used to create an effective coupling between these two NAMRs, and also to measure and control the two NAMRs. We have shown that two-mode squeezed states can be generated in a robust manner by this device, in analogy to the two-mode parametric down-conversion process in quantum optics. This two-mode down-conversion process offers a protocol of producing entanglement in two mechanical resonators in a solid state device, while previous proposals, see, e.g., Refs. 24, 25, and 49, were based on entanglement swapping by the assistance of photons. Our proposal might be promising for the experimental test of the existence of entangled states of macroscopic objects.

ACKNOWLEDGMENTS

F.N. was supported in part by the US National Security Agency (NSA), Army Research Office (ARO), Laboratory of Physical Sciences (LPS), and the National Science Foundation Grant No. EIA-0130383. C.P.S. was supported in part by the NSFC with Grant Nos. 90203018, 10474104, and 60433050; and the National Fundamental Research Program of China with Grant Nos. 2001CB309310 and 2005CB724508.

APPENDIX: HEISENBERG-LANGEVIN EQUATION FOR TWO NANOMECHANICAL RESONATORS

Using Eqs. (34a) and (34b), a solution of the expectation values $\langle b_L(t) \rangle$ and $\langle b_R(t) \rangle$ can be given as

$$\langle b_L \rangle = e^{-(1/2)\kappa_L t} [\langle b_L(0) \rangle \cosh(\xi t) - \langle b_R^\dagger(0) \rangle \sinh(\xi t)], \quad (\text{A1a})$$

$$\langle b_R \rangle = e^{-(1/2)\kappa_R t} [\langle b_R(0) \rangle \cosh(\xi t) - \langle b_L^\dagger(0) \rangle \sinh(\xi t)]. \quad (\text{A1b})$$

It is seen that below the thresholds $\xi < \kappa_L/2$ and $\xi < \kappa_R/2$ we have

$$\langle b_L \rangle = \langle b_R \rangle = 0. \quad (\text{A2})$$

The variance of the collective coordinates X_T can be evaluated by the expectation values of the bilinear operators of the two NAMRs. These are the expectation values of the quadratic operators of the left NAMR

$$L_1 = \langle b_L^2 \rangle, \quad L_3 = \langle b_L^{\dagger 2} \rangle, \quad (\text{A3a})$$

$$L_2 = \langle b_L^\dagger b_L + b_L b_L^\dagger \rangle, \quad (\text{A3b})$$

the expectation values of the quadratic operators of the right NAMR

$$R_1 = \langle b_R^2 \rangle, \quad R_3 = \langle b_R^{\dagger 2} \rangle, \quad (\text{A4a})$$

$$R_2 = \langle b_R^\dagger b_R + b_R b_R^\dagger \rangle, \quad (\text{A4b})$$

and the expectation values of the quadratic operators of both NAMRs

$$C_1 = \langle b_L b_R + b_R b_L \rangle = C_4^\dagger, \quad (\text{A5a})$$

$$C_2 = \langle b_L b_R^\dagger + b_R^\dagger b_L \rangle = C_3^\dagger. \quad (\text{A5b})$$

From Eq. (34) it is found that these expectation values satisfy a closed set of equations of motion.³⁵ To determine the values involving the expectation values of the products of the noise operators and the operators of the NAMRs, we rewrite Eqs. (34a) and (34b) and their corresponding Hermitian ones in the matrix form

$$\dot{\mathcal{B}} = -\mathcal{M}\mathcal{B} + \mathcal{F}, \quad (\text{A6})$$

where $\mathcal{B} = [b_L(t), b_L^\dagger(t), b_R(t), b_R^\dagger(t)]^T$ and $\mathcal{F} = [F_L(t), F_L^\dagger(t), F_R(t), F_R^\dagger(t)]^T$ are vectors, and $[\dots]^T$ represents the transpose operation. Here

$$\mathcal{M} = \begin{bmatrix} \frac{\kappa_L}{2} & 0 & 0 & \xi \\ 0 & \frac{\kappa_L}{2} & \xi & 0 \\ 0 & \xi & \frac{\kappa_R}{2} & 0 \\ \xi & 0 & 0 & \frac{\kappa_R}{2} \end{bmatrix}. \quad (\text{A7})$$

A formal solution of Eq. (A6) is given by

$$\mathcal{B}(t) = e^{-\mathcal{M}t}\mathcal{B}(0) + \int_0^t e^{-\mathcal{M}(t-t')}\mathcal{F}(t')dt'. \quad (\text{A8})$$

Multiplying the above equation by $\mathcal{F}^\dagger(t)$ from the right side, we obtain

$$\mathcal{B}(t)\mathcal{F}^\dagger(t) = e^{-\mathcal{M}t}\mathcal{B}(0)\mathcal{F}^\dagger(t) + \int_0^t e^{-\mathcal{M}(t-t')}\mathcal{F}(t')dt'\mathcal{F}^\dagger(t). \quad (\text{A9})$$

Since the operators of the NAMRs at the initial time $t=0$ are statistically independent of the noise operators, we have $\langle\mathcal{B}(0)\mathcal{F}^\dagger(t)\rangle=0$. Using the fact that the corresponding elements of the matrix of the left part of Eq. (A9) and those of the matrix of the right part of Eq. (A9) are equal, and combining the Markov approximation, we obtain

$$\langle b_L(t)F_L^\dagger(t)\rangle = \frac{\kappa_L}{2}, \quad (\text{A10a})$$

$$\langle b_R(t)F_R^\dagger(t)\rangle = \frac{\kappa_R}{2}. \quad (\text{A10b})$$

All other products of the operators of the two NAMRs and the noise operators are zero. Therefore, in the interaction picture, finally when the expectation values of these bilinear operators do not change with time, we obtain

$$L_1 = L_3 = R_1 = R_3 = C_2 = C_3 = 0 \quad (\text{A11})$$

and

$$L_2 = \frac{\kappa_-}{\kappa_+} + \frac{2\kappa_R}{\kappa_+}\Delta_\xi, \quad (\text{A12a})$$

$$R_2 = -\frac{\kappa_-}{\kappa_+} + \frac{2\kappa_L}{\kappa_+}\Delta_\xi, \quad (\text{A12b})$$

$$C_1 = C_4 = -\frac{4\xi}{\kappa_+}\Delta_\xi, \quad (\text{A12c})$$

with $\xi < \kappa_L/2$ and $\xi < \kappa_R/2$. Also, in the interaction picture, we have $\langle b_L(t)\rangle = \langle b_R(t)\rangle = 0$ after a sufficiently long time. Therefore, the variance of the collective coordinate X_T becomes

$$[\Delta(X_T)]^2 = \delta_L^2 L_2 + \delta_R^2 R_2 + \delta_L \delta_R (C_1 + C_4). \quad (\text{A13})$$

This provides the main result of Sec. III.

¹A. N. Cleland, *Foundations of Nanomechanics: From Solid-State Theory to Device Applications* (Springer-Verlag, Berlin, 2002).

²R. H. Blick *et al.*, *J. Phys.: Condens. Matter* **14**, R905 (2002).

³M. Blencowe, *Phys. Rep.* **395**, 159 (2004).

⁴K. Schwab and M. Roukes, *Phys. Today* **58** (7), 36 (2005).

⁵X. M. H. Huang, C. A. Zorman, M. Mehregany, and M. L. Roukes, *Nature* (London) **421**, 496 (2003).

⁶A. Gaidarzhy, G. Zolfagharkhani, R. L. Badzey, and P. Mohanty, *Phys. Rev. Lett.* **94**, 030402 (2005).

⁷K. C. Schwab, M. P. Blencowe, M. L. Roukes, A. N. Cleland, S. M. Girvin, G. J. Milburn, and K. L. Ekinci, *Phys. Rev. Lett.* **95**, 248901 (2005).

⁸A. Gaidarzhy, G. Zolfagharkhani, R. L. Badzey, and P. Mohanty, *Phys. Rev. Lett.* **95**, 248902 (2005).

⁹S. Savel'ev, X. Hu, and F. Nori, *New J. Phys.* **8**, 105 (2006).

¹⁰S. Savel'ev and F. Nori, *Phys. Rev. B* **70**, 214415 (2004).

¹¹N. Nishiguchi, *Phys. Rev. B* **68**, 121305(R) (2003).

¹²S. Savel'ev, A. L. Rakhmanov, X. Hu, A. Kasumov, and F. Nori, *Phys. Rev. B* **75**, 165417 (2007).

¹³A. D. Armour, M. P. Blencowe, and K. C. Schwab, *Phys. Rev. Lett.* **88**, 148301 (2002).

¹⁴Y. D. Wang, Y. B. Gao, and C. P. Sun, *Eur. Phys. J. B* **40**, 321 (2004).

¹⁵P. Zhang, Y. D. Wang, and C. P. Sun, *Phys. Rev. Lett.* **95**, 097204 (2005).

¹⁶C. P. Sun, L. F. Wei, Y.-X. Liu, and F. Nori, *Phys. Rev. A* **73**, 022318 (2006).

¹⁷L. F. Wei, Y.-X. Liu, C. P. Sun, and F. Nori, *Phys. Rev. Lett.* **97**, 237201 (2006).

¹⁸E. Buks, E. Arbel-Segev, S. Zaitsev, B. Abdo, and M. P. Blencowe, arXiv:quant-ph/0610158 (unpublished).

¹⁹F. Xue, Y. D. Wang, C. P. Sun, H. Okamoto, H. Yamaguchi, and K. Semba, *New J. Phys.* **9**, 35 (2007).

²⁰F. Xue, L. Zhong, Y. Li, and C. P. Sun, *Phys. Rev. B* **75**, 033407 (2007).

²¹X. Zhou and A. Mizel, *Phys. Rev. Lett.* **97**, 267201 (2006).

²²P. Rabl, A. Shnirman, and P. Zoller, *Phys. Rev. B* **70**, 205304 (2004).

²³R. Ruskov, K. Schwab, and A. N. Korotkov, *Phys. Rev. B* **71**, 235407 (2005).

²⁴S. Mancini, V. Giovannetti, D. Vitali, and P. Tombesi, *Phys. Rev. Lett.* **88**, 120401 (2002).

²⁵S. Pirandola, D. Vitali, P. Tombesi, and S. Lloyd, *Phys. Rev. Lett.* **97**, 150403 (2006).

²⁶J. Eisert, M. B. Plenio, S. Bose, and J. Hartley, *Phys. Rev. Lett.* **93**, 190402 (2004).

²⁷X. Hu and F. Nori, *Phys. Rev. Lett.* **76**, 2294 (1996).

²⁸X. Hu and F. Nori, *Phys. Rev. B* **53**, 2419 (1996).

²⁹X. Hu and F. Nori, *Phys. Rev. Lett.* **79**, 4605 (1997).

³⁰X. Hu and F. Nori, *Physica B* **263**, 16 (1999).

- ³¹J. Q. You and F. Nori, *Phys. Today* **58** (11), 42 (2005).
- ³²G. Wendin and V. Shumeiko, arXiv:cond-mat/0508729 (unpublished).
- ³³A. Zavatta, S. Viciani, and M. Bellini, *Science* **306**, 660 (2004).
- ³⁴P. K. Day, H. G. LeDuc, B. A. Mazin, A. Vayonakis, and J. Zmuidzinas, *Nature (London)* **425**, 817 (2003).
- ³⁵M. O. Scully and M. S. Zubairy, *Quantum Optics* (Cambridge University Press, Cambridge, 1997).
- ³⁶A. Gaidarzhy, G. Zolfagharkhani, R. L. Badzey, and P. Mohanty, *Appl. Phys. Lett.* **86**, 254103 (2005).
- ³⁷S. O. Valenzuela, W. D. Oliver, D. M. Berns, K. K. Berggren, L. S. Levitov, and T. P. Orlando, *Science* **314**, 1589 (2006).
- ³⁸M. D. LaHaye, O. Buu, B. Camarota, and K. C. Schwab, *Science* **304**, 74 (2004).
- ³⁹J. N. Munday, D. Iannuzzi, Y. Barash, and F. Capasso, *Phys. Rev. A* **71**, 042102 (2005).
- ⁴⁰J. N. Munday, D. Iannuzzi, and F. Capasso, *New J. Phys.* **8**, 244 (2006).
- ⁴¹F. Capasso, J. N. Munday, D. Iannuzzi, and H. B. Chan, *IEEE J. Sel. Top. Quantum Electron.* **13**, 400 (2007).
- ⁴²K. B. Cooper, M. Steffen, R. McDermott, R. W. Simmonds, S. Oh, D. A. Hite, D. P. Pappas, and J. M. Martinis, *Phys. Rev. Lett.* **93**, 180401 (2004).
- ⁴³A. Naik, O. Buu, M. D. LaHaye, A. D. Armour, A. A. Clerk, M. P. Blencowe, and K. C. Schwab, *Nature (London)* **443**, 193 (2006).
- ⁴⁴A. Schliesser, P. Del'Haye, N. Nooshi, K. J. Vahala, and T. J. Kippenberg, *Phys. Rev. Lett.* **97**, 243905 (2006).
- ⁴⁵D. Kleckner and D. Bouwmeester, *Nature (London)* **444**, 75 (2006).
- ⁴⁶S. Gigan, H. R. Bohm, M. Paternostro, F. Blaser, G. Langer, J. B. Hertzberg, K. C. Schwab, D. Bauerle, M. Aspelmeyer, and A. Zeilinger, *Nature (London)* **444**, 67 (2006).
- ⁴⁷M. Poggio, C. L. Degen, H. J. Mamin, and D. Rugar, *Phys. Rev. Lett.* **99**, 017201 (2007).
- ⁴⁸E. K. Irish and K. C. Schwab, *Phys. Rev. B* **68**, 155311 (2003).
- ⁴⁹J. Zhang, K. Peng, and S. L. Braunstein, *Phys. Rev. A* **68**, 013808 (2003).